

Electron Heat Transport in ASDEX Upgrade: Experiment and Modelling

F. Ryter 1), G. Tardini 1), F. De Luca 2), H.-U. Fahrbach 1), F. Imbeaux 3), A. Jacchia 4), K.K. Kirov 1), F. Leuterer 1), P. Mantica 4), A.G. Peeters 1), G. Pereverzev 1), W. Suttrop 1) and ASDEX Upgrade Team 1)

1) Max-Planck-Institut für Plasmaphysik, EURATOM-IPP Association, Germany

2) INFN and Dipartimento di Fisica, Università degli Studi di Milano, Milano, Italy

3) DRFC, Association Euratom-CEA, CEA-Cadarache, France

4) Istituto di Fisica del Plasma, Associazione EURATOM-ENEA-CNR, 20133 Milano, Italy

e-mail contact of main author: ryter@ipp.mpg.de

Abstract. Electron heat transport is studied in ASDEX Upgrade with Electron Cyclotron Heating for steady-state and power modulation. Experiments with varying core heat flux at constant edge flux allow a detailed determination of the transport characteristics.

1. Experimental set-up and methods of analysis

Electron heat transport has been investigated [1, 2] in the ASDEX Upgrade tokamak ($R=1.65$ m, $a=0.5$ m) using the Electron Cyclotron Heating system, composed of 4 beams which can be deflected independently by mirror launchers. The width of the beam is narrow, ≈ 3 cm, and the single-pass absorption 100%. The electron temperature is provided by the 60 channel ECE heterodyne radiometer, with a spatial resolution of 1 to 3 cm and a bandwidth of ≈ 30 kHz, and by the Thomson scattering with 16 channels. These two diagnostics agree within $\pm 10\%$. The ion temperature is measured here with two neutral particle analyzers with their line of sight viewing at the center and at mid-radius. At low density as here, these T_i values are quite reliable. The experimental studies of electron heat transport have been performed in ASDEX Upgrade by combinations of the steady-state and temperature modulation methods. This yields the usual power balance heat conductivity χ_e^{PB} . The propagation of the heat pulses excited by the power modulation is characterized by [3]:

$$\chi_e^{HP} = \chi_e^{PB} + \frac{\partial \chi_e}{\partial \nabla T_e} \nabla T_e \quad (1)$$

It is derived experimentally from Fourier transform of T_e , according to the expressions for slab geometry [3] and with corrections for cylindrical geometry and density gradient [4].

2. Basics on electron heat transport

Studies in ASDEX Upgrade [1, 2] and other tokamaks [5, 6, 7] suggest that electron heat transport is governed by turbulence increasing above a threshold $(\nabla T_e / T_e)_{crit} = (1/L_{T_e})_{crit}$, named κ here, and below which heat transport is very small (χ_0). This is suggested by turbulence theory based on Trapped Electron Modes [8] and Electron Temperature Gradient modes [9]. These instabilities have a respective threshold in $1/L_{T_e}$, dimensionless R/L_{T_e} . As a consequence, the temperature profiles react weakly to changes of the heating profile: “profile resilience” discussed for 2 decades. In fact, the temperature profiles exhibit similar values of R/L_{T_e} in toka-

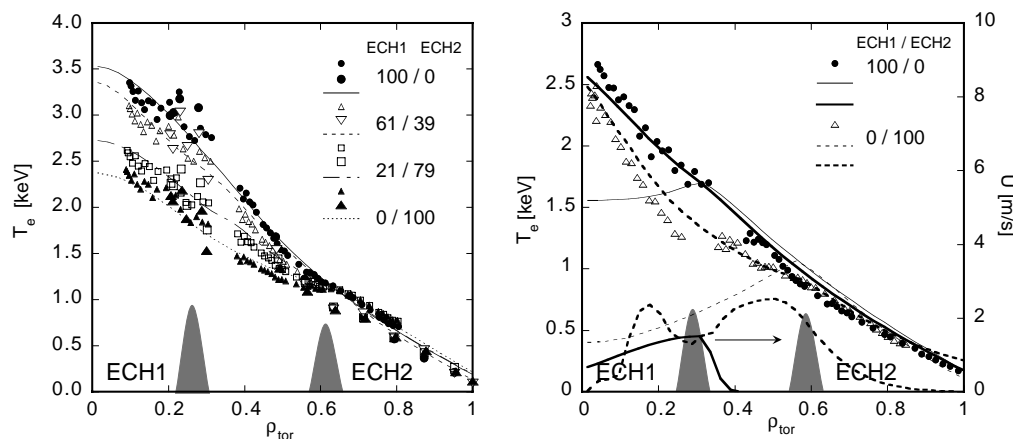


Figure 1: T_e profiles in the experiments with heat flux variation by ECH in the confinement region with constant edge flux ($P_{ECH1} + P_{ECH2} = 1.3\text{MW}$). The respective percentage with respect to the total ECH power is indicated. Left $I_p = 800$ kA, right $I_p = 400$ kA. Small symbols for ECE, large for Thomson scattering, lines for modeling. On the right plot the thick lines are from modeling with inward convection U , also plotted with the corresponding line type.

maks [5]. An analytical transport model has been developed and successfully tested on ASDEX Upgrade data [10]. This model, extended now with a q dependence, reads:

$$\chi_e = \chi_0 + q \cdot \lambda \cdot T_e^{3/2} (\nabla T_e / T_e - \kappa) H(\nabla T_e / T_e - \kappa) \quad (2)$$

where q is the safety factor, λ and κ are coefficients to be adjusted, H is the Heaviside function. The $T_e^{3/2}$ factor takes into account the Gyro-Bohm dependence expected from transport driven by micro-turbulence. It introduces a decrease of χ_e with radius, not observed in the experiments, which is by $q(r)$ which increases towards the edge. We will show below that introducing q also allows to model correctly discharges at different plasma current without changing λ . The factor $q \cdot \lambda \cdot T_e^{3/2}$ determines the stiffness of the profiles at each radius. In the remaining of this paper, the units are mks except keV for the temperatures. Using Eq. 1, the expression for χ_e^{HP} can be derived explicitly for the model described by Eq. 2:

$$\chi_e^{HP} = \chi_0 + q \cdot \lambda \cdot T_e^{3/2} (2\nabla T_e / T_e - \kappa) H(\nabla T_e / T_e - \kappa) \quad (3)$$

assuming that χ_0 does not depends on ∇T_e . It shows the important property that χ_e^{HP} increases in a step largely above χ_0 as soon as $\nabla T_e / T_e$ is larger than κ , whereas χ_e^{PB} increases continuously with $\nabla T_e / T_e - \kappa$, see [10] and Fig. 2. The validity of the model is supported by the good results obtained in ASDEX Upgrade with Weiland's model [8] in ECH heated plasmas [11].

3. Experiment: Variation of the electron heat flux at constant edge flux

According to the considerations of Sect. 2, it is essential in transport studies to vary $\nabla T_e / T_e$ in the confinement region at constant edge temperature. This was achieved in new experiments at ASDEX Upgrade where we varied the electron heat flux in the confinement region ($0.35 \leq \rho_t \leq 0.65$) by one order of magnitude while keeping the heat flux at the plasma edge ($\rho_t \geq 0.65$) constant, ρ_t being the normalized toroidal flux radius. For this purpose, we deposited the ECH power at $\rho_1 \approx 0.35$ and $\rho_2 \approx 0.65$ with the respective intensities P_{ECH1} and P_{ECH2} . These were varied while keeping $P_{ECH1} + P_{ECH2}$ constant at about 1.3 MW. The

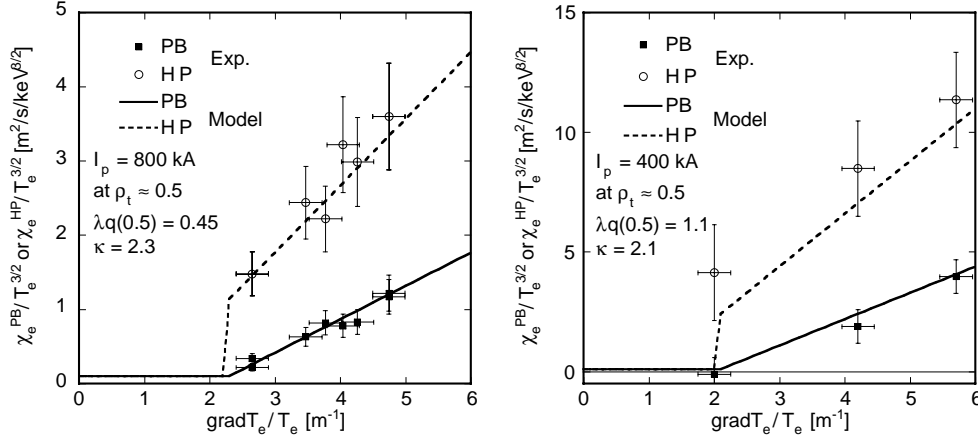


Figure 2: Results from power balance and heat pulse analysis at $\rho_t \approx 0.5$, for the discharges at $I_p = 800$ kA and $I_p = 400$ kA. The lines are given by the model from Eq. 2 for which the values of κ and $q \cdot \lambda$ are indicated in the figure.

discharges were L modes at low density $\bar{n}_e = 2 \cdot 10^{19} m^{-3}$ to reduce the electron-ion energy transfer. Modulation of P_{ECH1} or P_{ECH2} yields χ_e^{HP} . We performed two series of discharges at different values of plasma current, 800 kA and 400 kA, but at the same magnetic field of 2.35 T required by the ECH. Due to the high q value the discharges at 400 kA were not sawtoothing. Some steady-state temperature profiles are shown in Fig. 1. A clear variation of ∇T_e and $\nabla T_e/T_e$ could be achieved, which is not the case when central heating only is varied because the edge temperature increases with heating power [1].

The results of power balance and transient transport at $\rho_t \approx 0.5$ are shown in Fig. 2. The χ_e values are divided by the $T_e^{3/2}$. Note the different scales: transport is much larger at low current. A linear fit through the power balance data (solid line in the plots), neglecting the very small contribution from χ_0 , yields the values of $\lambda \cdot q(0.5)$ and κ at $\rho_t = 0.5$ indicated in each plot. The values for κ are very similar whereas those for $\lambda \cdot q(0.5)$ differ significantly. The simulations described below and the analysis from MHD equilibrium show that at $\rho_t \approx 0.5$ q varies by a factor of about 2 between the two series, showing that λ remains almost constant around 0.4. Using these values for $\lambda \cdot q(0.5)$ and κ we can calculate the corresponding χ_e^{HP} given by Eq. 3. The results, dashed lines in Fig. 2, agrees well with the experimental data.

These values of λ and κ were then taken for transport simulations with the ASTRA code using Eq. 2 as transport model. The results, lines in Fig. 1, agree very well with the experimental data over the whole radius for all the 800 kA cases. At 400 kA the simulated T_e profiles tend to be hollow in the region inside the ECH deposition, thin lines in the figure. There, the losses from the electron channel to the ions cannot be compensated by the Ohmic power. The analysis is delicate there because transport and fluxes are very low. The possible influence of convection, off-diagonal transport coefficients, spurious ECH power or particular Z_{eff} profile to explain the peaked T_e profiles is under investigation [12]. If convection is assumed, giving the thick lines in the 400 kA plot, it has to be peaked inside the ECH deposition with a maximum of about 2 m/s, which is small and does not directly influence the results of the modulation at the frequency of 30 Hz used here. Convection and off-diagonal terms with the right sign indeed exist in ITG/TEM physics [8, 12]. Assuming spurious ECH power, only 3% to 5% are required.

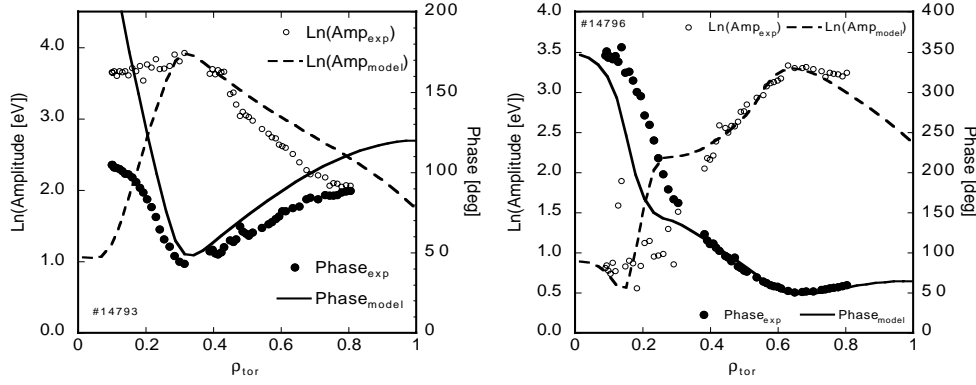


Figure 3: Amplitude and phase of the T_e modulation for the two extreme cases of Fig. 1, $P_{ECH1} = 100\%$ (left) or $P_{ECH2} = 100\%$ (right). The points are the data, the lines the empirical model.

The simulations also include the power modulation made in the experiment. The results of the Fourier transform of the experimental and modeled T_e are illustrated in Fig. 3 by the two extreme cases with central or edge heating at $I_p = 800$ kA. The agreement is quite satisfactory. The other cases at 800 kA give comparably good results. The results from the 400 kA cases with full or partial central heating are acceptable but yield a value for χ_e^{HP} which is about 30% too low. The pure off-axis case is not well reproduced which due to the discrepancy between the experimental and simulated steady-state profiles caused by the negative power balance mentioned above.

Independently of the simulations, in the frame of our model the experimental T_e profiles the in off-axis cases are expected to be just above but very close to the threshold in the region between plasma center and ECH2 deposition, due to the low heat flux there. Thus, R/L_{T_e} deduced from the T_e profiles in this region is expected to yield a direct measurement of $(R/L_{T_e})_{crit}$ to be compared with theoretical values. This is illustrated in Fig. 4 where the experimental R/L_{T_e} deduced from the respective T_e profiles in the 800 kA and 400 kA off-axis cases are compared with the threshold $(R/L_{T_e})_{crit}$ for TEM and ETG driven turbulence yielded by the formulas given in [8] and [9] respectively. The threshold for TEM depends on the destabilizing fraction of trapped electrons and on the stabilizing R/L_{n_e} [8]. In our cases with flat density profiles the latter occurs only at the plasma edge, as shown by Fig. 4. The TEM threshold is in good agreement with the experimental curve in the region inside of ECH2, at both 800 kA and 400 kA. At 800 kA, the central sawtooth region must be excluded, at 400 kA the requirement of a zero derivative on the axis forces the T_e profile below the threshold. Modulation data indicate that at 400 kA R/L_{T_e} drops below the threshold in the region $0.25 \leq \rho_t \leq 0.4$ as in Fig. 4. The simulation with the model (Eq. 2) yields better results when the TEM threshold is used instead of a constant κ . In contrast, the ETG threshold at 800 kA is much higher than the experimental R/L_{T_e} . Its formula consists of 2 factors [9]: $(R/L_{T_e})_{ETG} \propto (1 + Z_{eff} T_e/T_i)(1.33 + 1.91s/q)$, where s is the magnetic shear. The values of Z_{eff} are estimated to lie between 1.6 and 2 in the plasma core and to be quite similar for all the discharges. We used $Z_{eff} = 1.6$ in the formula to minimize the ETG threshold. In our experiments T_e/T_i decreases from about 2.5 at 800 kA to 1.5 at 400 kA, and s/q decreases by about a factor 2 from 800 kA to 400 kA. This explains the reduction of the ETG threshold with plasma current. At 400 kA the ETG threshold is just above the experimental values of R/L_{T_e} and cannot be completely excluded in this case.

As mentioned above, a property of the model is the step of by χ_e^{HP} at the threshold, which is a check for the model and a useful monitor: above or below the threshold. We have started to

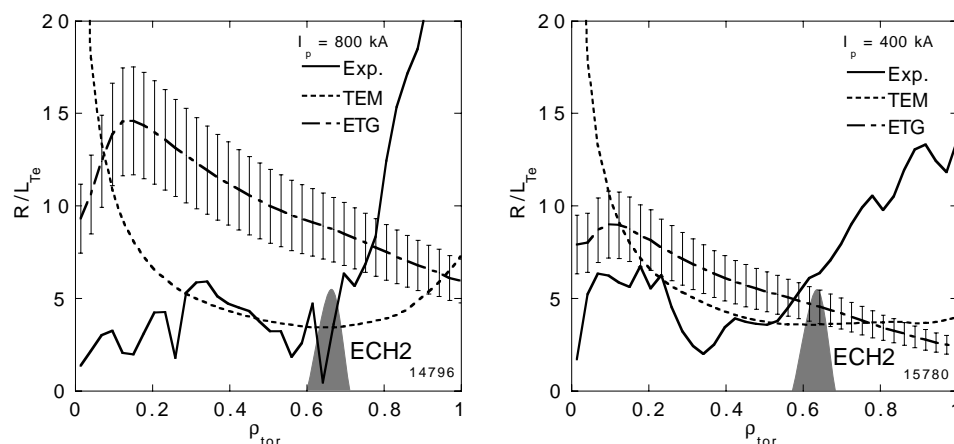


Figure 4: Experimental profile of R/L_{T_e} and threshold values for TEM and ETG driven turbulence. The error bars on the ETG threshold correspond to a simultaneous variation up to $\pm 20\%$ of T_e/T_i and s/q .

investigate in detail the behavior of χ_e^{HP} around the threshold.

As already shown for others discharges [11], here also at 800 kA the ITG/TEM Weiland model [8] gives for both the steady-state and modulation data quite good results, which are very similar to those obtained with the empirical model. However the 400 kA cases are poorly reproduced, the stiffness factor is too low by about 50%, hence electron transport also. For central heating this is reflected in T_e profiles which are too high and too peaked and in values χ_e^{HP} which are correspondingly too low.

Concluding, this study shows that the T_e profiles are moderately stiff. Steady-state and modulation data are well simulated with a single transport model involving a critical temperature gradient length. The experimental threshold behavior suggests TEM turbulence being present.

Acknowledgement

We are glad to acknowledge very fruitful discussions with X. Garbet. We are grateful to J. Weiland for helpful discussions and for having provided us with his ITG/TEM transport code. It is a pleasure to thank the ASDEX Upgrade and ECRH technical groups for their excellent support.

References

- [1] RYTER, F. et al., Phys. Rev. Lett. **86** (2001) 2325.
- [2] RYTER, F. et al., Phys. Rev. Lett. **86** (2001) 5498.
- [3] LOPES CARDOZO, N. J., Plasma Phys. Contr. Fusion **37** (1995) 799.
- [4] JACCHIA, A. et al., Phys. Fluids **B 3** (1991) 3033.
- [5] RYTER, F. et al., Plasma Phys. Controlled Fusion **43** (2001) A323.
- [6] HOANG, G. T. et al., Phys. Rev. Lett. **87** (2001) 125001.
- [7] MANTICA, P. et al., This Conference, paper EX/P1-04 (2002).
- [8] NORDMAN, H. et al., Nucl. Fusion **30** (1990) 983.
- [9] JENKO, F. et al., Phys. Plasmas **8** (2001) 4096.
- [10] IMBEAUX, F. et al., Plasma Phys. Controlled Fusion **43** (2001) 1503.
- [11] TARDINI, G. et al., Nucl. Fusion **42** (2002) L11.
- [12] MANTICA, P. et al., Investigation of heat pinch effects in tokamak plasmas, TTF Workshop (2002).